Review

Research status and future perspectives of low dimensional electromagnetic wave absorption materials

Huaping Xu [‡,1,2], Tao Tang [‡,1,2], Zengming Man [1,*], Xiaofeng Wu [3], Haiqiang Zhao [3], Xiaohui Liang [4], Chuanying Li [1,2]

[1] School of Materials Science and Engineering, Zhejiang Sci-Tech University, Hangzhou, 310018, China.
[2] School of Chemistry and Chemical Engineering, Key Laboratory of Surface & Interface Science of Polymer Materials of Zhejiang Province, Zhejiang Sci-Tech University, Hangzhou, 310018, China
[3] Zhejiang Linix Motor CO LTD, Dongyang City, 322118, P. R. China.
[4] Hangzhou Dianzi University, Hangzhou 310018, P. R. China.
* Correspondence: zmman@zstu.edu.cn (Z.M.)

Abstract: Highly efficient, broadband and distinctively structured electromagnetic wave (EMW) absorption materials exhibit huge exceptions with multi-functions in both military and civilian fields. Searching the relationship between structural and EMW performance is beneficial to develop outstanding microwave absorption materials, and has become an attractive research topic. In this study, we briefly reviewed the different EMW absorption mechanisms and key influence factors, then, present the latest developments in low-dimensional (LD) EMW absorption materials. We provide a comprehensive discussion of remarkable examples and summarize the main information related to the structure-function relationship of dimensional design and structural engineering in order to facilitate the rapid evolution of this fascinating field.

Keywords: electromagnetic wave absorption; attenuation mechanism; low-dimensional materials

1. Introduction

Electromagnetic wave (EMW) has a wide range of application scenarios, and has now penetrated into the aspect of communication, entertainment, medical and scientific research of our life and plays a vital role in the field of technology and science.[1] [2-3] With civilizations flourishing, EMW functional materials and devices bring great benefit to human activities covering from 10^3 to 10^{23} Hz in EMW spectrum.[4] As shown in Figure 1a, an ultralong wave of $\lambda = 10^4$ -10^5 m is used for maritime communications and navigations; a medium-short wave of λ = 1-10^3 m is usually applied to televisions, radios, and cell phones, which let us know everything without going out; centimeter wave of λ =10^{-3}-10^{-2} m is employed in global position system positioning and satellite communications. Furthermore, terahertz wave, infrared wave, and X-rays have made brilliant achievements in detecting and imaging, extensively used in various fields, ranging from security precaution to medicine and military.[5-6] However, the release of EMW will cause harmful issues to human beings and environment.[7-9] For instance, EMW can be used to detect the signals of warplanes, missiles, ships, and other military equipment, scarifying their concealment and survivability (Figure 1b).[10-11] At the same time, EMW absorbent will disturb the electronic devices, lead to the increased failure rate and reduced stability and reliability (Figure 1c). For humans, long-term exposure to electromagnetic waves may cause headaches, insomnia, neurasthenia, muscle fatigue. In high intensity electromagnetic radiation, the human body may also appear nausea, syncope, arrhythmia, and may increase the incidence of diseases such as cancer and infertility (Figure 1d). Hence, tremendous researchers have focused on developing novel and efficient EM wave absorbing materials to deal the rising electromagnetic pollution issues.

The development of high-efficiency and high-potential EMW functional materials and devices will bring more surprise, especially in low dimension (LD) and nanoscale.[12-13] New physical effects and EMW properties, as well as multivariate and miniaturized EMW devices, constantly refresh

Preprints (www.preprints.org) | NOT PEER-REVIEWED | Posted: 15 June 2023 doi:10.20944/preprints202306.1136.v1

the world, bringing infinite vitality to future development of various fields.[14-15] Low-dimensional materials have recently emerged as a class of potentially absorber with manageable conductivity, rich surface group, and unique structure lead to the enhanced activity and increased stability.[16] These materials are smaller than 100 nm in at least one dimension, and examples include 0D nanoparticles and quantum dots; 1D nanotubes, nanoribbons and nanowires; and 2D nanosheets.[17-19] The dimensional reduction of bulk materials may impose quantum confinement on the electronic density of states at the nanoscale limit, which modifies the electronic structure. In this study, we take some low-dimensional EMW functional materials as examples, including quantum dots, graphene, MXene, and transition metals and compounds. We briefly introduce the mechanisms of electromagnetic wave absorption, and listed the recently developed electromagnetic wave absorption materials. Further, we demonstrate various EM functional devices, predicting the most prospective direction in the future.[20-21]

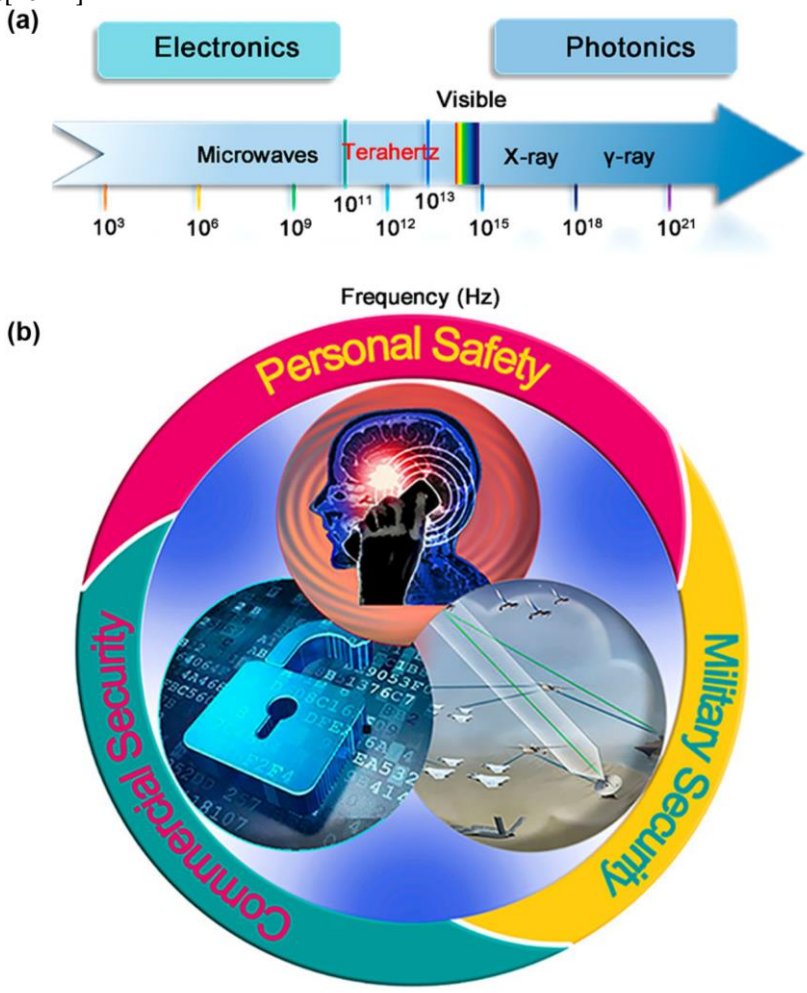

Figure 1. (a) location of THz in electromagnetic spectrum. (b) Harm of electromagnetic waves.

2. Microwave absorption mechanisms

EMW will be reflected, absorbed, or penetrated when incident on the surface of a material (Figure 2a). EMW absorption requires the energy of electromagnetic wave is transformed into other energy, which less energy is reflected or permeated through the materials.[22] Ideal EMW absorption materials should possess proper impedance matching and strong magnetic/dielectric loss. Based on impedance matching mechanism, the material with low conductivity is not applicable, where large amount of EMW were reflected and penetrated (Figure 2a, left part). On the other hands, high conductivity led to a skin depth area and most EMW was reflected (Figure 2a, right part).[23-24] Therefore, the EMW absorption effect is optimization when the permeability is equal to the permittivity of

Preprints (www.preprints.org) | NOT PEER-REVIEWED | Posted: 15 June 2023 doi:10.20944/preprints202306.1136.v1

material, making less EMW was reflected, which would get better wave absorption effect. The EMW absorption ability was often indicated by the reflection loss (RL):

$$R_l=-20\log\left|\frac{Z_{in}-1}{Z_{in}+1}\right| \quad (1)$$

$$Z_{in}=Z_0\sqrt{\frac{\mu_r}{\varepsilon_r}}\tanh\left[j\frac{2\pi df}{c}\sqrt{\mu_r\varepsilon_r}\right] \quad (2)$$

where Z_0, Z_{in}, f, d, and c represent the impedance of the free space, impedance of incident wave, real part of permeability, frequency of EM wave, thickness of material, and light speed, respectively.

The RL < -10 dB and -20 dB represent that 90% and 99% EMW are absorbed, respectively. The EMW attenuation mechanisms corresponding to materials of different dimensions mainly include conductivity loss, polarization loss, magnetic loss, and multiple scattering and reflection (Figure 2b-e).[25-27]

2.1. Conductivity Loss

Dielectric loss is usually determined by electric conduction loss, polarization relaxation, and multi-reflection and scattering. Conduction loss mainly results from charge transfer and plays an important role in EMW shielding and absorption.[28-29] The electron transport through the micro-current network includes directionally migrating in one layer and hopping across the defects or interface between layers under an applied electric field (Figure 2b).[30] In addition, hopping conduction depends on the temperature, and electrons can be activated at high temperatures, increasing the carrier concentration and conduction loss.[31] More hopping electrons will jump across the interface with the increasing temperature, attributed to the enhanced microcurrent and the hopping conductivity. Moreover, high filler loading will also benefit to form a conduction pathway and thus harvest EMW into thermal energy. In addition, the long-range oriented structure of the conductive network leads to rapidly attenuate EMW in multiple resistance networks.[32]

2.2. Polarization Relaxation

Polarization relaxation is another significant factor in the dielectric loss of materials. The loss is primarily caused by two types of polarization: intrinsic and extrinsic polarization. Intrinsic polarization arises from defects, functional groups, and lattice vacancies, generating dipoles that dissipate energy as they reorient themselves towards the direction of the EMW field.[33-34] Extrinsic polarization is dependent on the interfacial polarization, which is crucial for the design of efficient EMW shielding and absorption materials by integrating multiple dielectric/magnetic components with heterostructures (as shown in Figure 2c).[35] The resulting interfacial polarization has a significant impact on the overall dielectric losses.[36-37]

2.3. Magnetic Effect

The magnetic loss in materials is primarily attributed to three key factors of the eddy current effect, natural resonance, and exchange resonance consist of the magnetic loss, and influence the conversion of EMW energy into thermal energy.[38-40] The eddy current loss can be mathematically expressed as:

$$\mu''=2\pi\mu_0(\mu')^2\sigma d^2 f/3 \quad (3)$$

where μ_0 is the permeability of vacuum, f is the frequency, σ is the electrical conductivity, and d represents the thickness of the materials. The exchange resonance happens at a high frequency (>10 GHz), while the natural resonance occurs at a lower frequency (2-10 GHz). Additionally, the natural resonance is linked to the anisotropic field of magnetic particles. Smaller magnetic particles create stronger anisotropic fields, which allows the resonant frequency to be adjusted by modifying the anisotropic field. This ability to tune the anisotropic field is particularly useful in applications that necessitate absorption at specific frequencies.[36]

The presence of magnetic metal oxide nanoparticles generates eddy currents and magnetic resonance, contributing to magnetic loss, as shown in Figure 2c.[27] Composites made by combining dielectrics and magnets can achieve magnetoelectric synergy, enabling a matched characteristic impedance and strong attenuation capability.[41] This reduces surface reflection of the EMW and can contribute to minimum reflection loss (RL_{min}) values with a thinner matching thickness. The complex permittivity (ε_r) and complex permeability (μ_r) of the composite can be readily regulated by varying the magnetic filler content to facilitate impedance matching. Furthermore, increasing the number of

Preprints (www.preprints.org) | NOT PEER-REVIEWED | Posted: 15 June 2023 doi:10.20944/preprints202306.1136.v1

heterointerfaces intensifies polarization loss, leading to improved attenuation and absorption of electromagnetic waves in a broader frequency range in electromagnetic devices.

2.4. Multireflection and Scattering

2D materials possess exceptional properties, such as being ultra-thin, flexible, and corrugated, which increases the propagation paths for EMW inside the material, as demonstrated in Figure 2d.[13] This corrugated structure results in the scattering of EMW, facilitating multiple internal reflection modes and improving attenuation remarkably. Excitingly, interfacial scattering from heterostructures is a potent approach to bolster EMW energy dissipation. Interfacial engineering is typically observed in core-shell heterostructures, some ternary heterostructures, and a porous hierarchical architecture that can further promote the interfacial scattering effect.[37, 42] This is a promising generalizable strategy for a wide range of graphene-based assemblies, including films, fabrics, and composites.

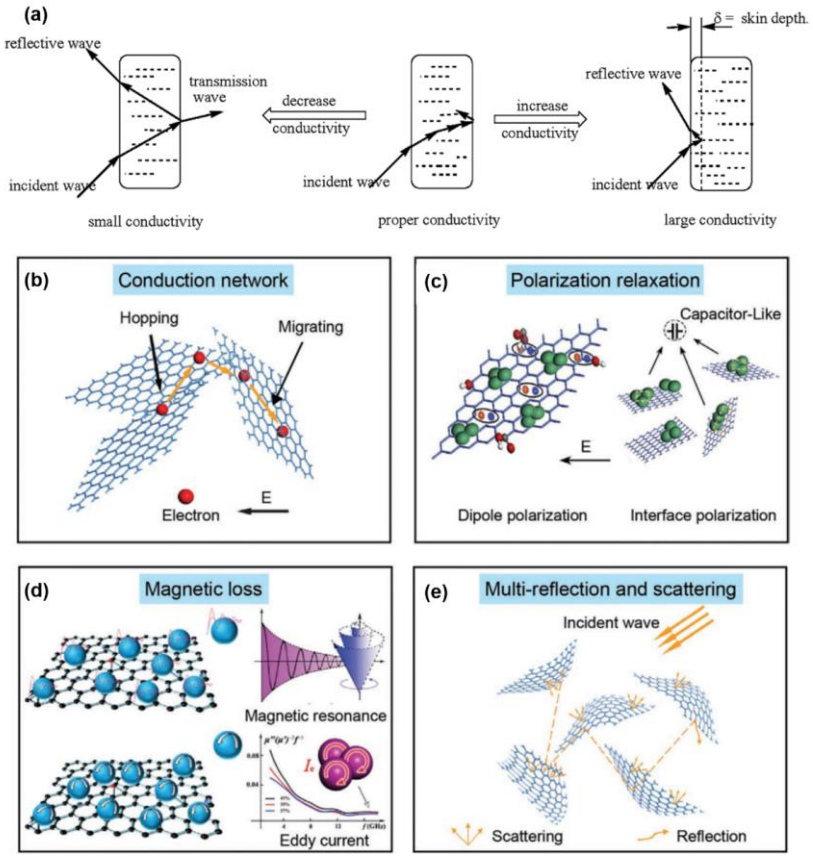

Figure 2. (a) EM wave attenuation mechanisms of graphene-based materials. (b) Conductivity Loss mechanism. (c) Polarization Relaxation Loss mechanism. (d) Magnetic Effect Loss mechanism. (e) Multireflection and Scattering Loss mechanism.

3. Low-dimensional EMW absorption materials

Low-dimensional materials are longitudinal size (on the nanoscale) significantly smaller than either of their lateral dimensions or thickness, formed at the nanoscale level. These materials have different dimensions, involving one-dimensional nanowires, two-dimensional materials such as graphene, phosphorus, and transition metal dichalcogenides and three-dimensional nanoporous materials. Low-dimensional materials possess a structurally unique feature, characterized by a high surface area to volume ratio, leading to excellent electrical, optical, mechanical, thermal, and chemical properties. Furthermore, these materials exhibit quantum size effects, which impart distinctive properties. The absorption properties of electromagnetic waves are significantly influenced by factors such as electronic and magnetic properties, size, morphology, and structure of the material, as guided

Preprints (www.preprints.org) | NOT PEER-REVIEWED | Posted: 15 June 2023 doi:10.20944/preprints202306.1136.v1

by the mechanism of electromagnetic wave absorption. Apart from intrinsic electromagnetic characteristics, the morphology and microstructure of the material also play a critical role in determining the performance of electromagnetic wave absorption. Therefore, while considering the absorption properties of electromagnetic waves of a particular material, it is important to consider not only its intrinsic electromagnetic properties but also its morphology and microstructure.

3.1. 0D EMW materials

Quantum dots (QDs) are zero-dimensional nano-level semiconductors,[43] and can reach a high dielectric constant of 144, which was ascribed to Maxwell Wagner-Sillars or interfacial polarization.[44] Moreover, the quantum size effect is a foregrounded strategy to design and fabricate excellent electromagnetic microwave absorption materials. Prof. Wu rational designed $ZnFe_2O_4$ QDs coated by hybrid amorphous carbon as effective EMW absorption materials.[45] The particle size of $ZnFe_2O_4$@C mainly concentrated in 3.89 nm, which the microstructure and morphology characteristics were observed by TEM images in Figure 3a. $ZnFe_2O_4$ delivered high magnetic loss, and facilitated complex permittivity/permeability absorbing property which was optimized by carbon coting layer.[46] Indisputably, ascribed to the small size effect and multiple heterointerface, $ZnFe_2O_4$ reached a RL_{min} of -40.68 dB at the thickness 2.5 mm. On the contrary, $ZnFe_2O_4$ and $ZnFe_2O_4$-NH_3 almost showed noneffective EM absorb response.

When $|Z_{in}/Z_0|$ reaches to 1, $ZnFe_2O_4$@C has the greatest reflection loss, which indicating the reflection loss at different thicknesses is governed by the interplay between impedance matching and attenuation constant,[47] shown in Figure 3c. Additionally, $ZnFe_2O_4$@C exhibits an effective bandwidth of up to 13.92 GHz (4.08-18 GHz, where the thickness is 1.5-5 mm). This ideal impedance matching allows the construction of thinner EM absorption materials, while the high attenuation constant contributes to more effective energy loss. Moreover, heterogeneous structures are known to have excellent properties for conducting, polarizing, and enhancing magnetic loss in materials.[48-49] Michel reported polypyrrole (PPy)/carbon quantum dots (CQDs) heterostructures microwave absorbers (MA).[50] The proper addition of CQDs to PPy enhances the dielectric loss behavior, resulting in the enhanced microwave absorption performance of PPYCQD200, respectively. In Figure 3d, PPyCQD200 exhibits a high EM absorption ability of -32.68 dB at 4.75 mm thickness and a bandwidth of 1.35 GHz around the matching frequency of 4.6 GHz. However, there is a trade-off relationship between RL_{min} and effective bandwidth. The best impedance matching occurs for sample at 25% loading percentage, overload of PPY results in heavier EM absorber and decayed absorption performance. These results suggest the fabricated of heterostructure will synergistically enhance the EM absorption properties.

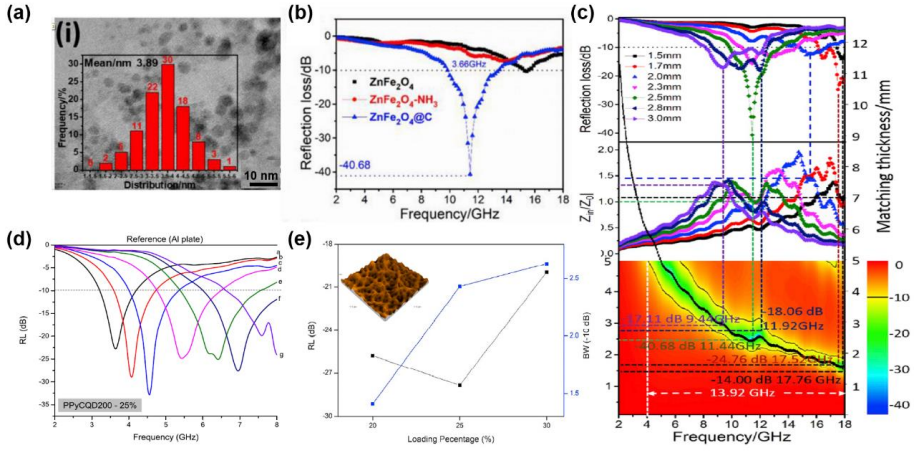

Figure 3. (a) TEM images of $ZnFe_2O_4$@C (insert: particle size distribution). (b) The RL value of $ZnFe_2O_4$@C at 2.5 mm. (c) Simulation of RL values and the impedance matching versus different frequency and thicknesses of $ZnFe_2O_4$@C. (d) RL curves of PPyCQD200 with loading percentage 25% at 3.5-6.0 nm. (e) RL_{min} and bandwidth at different loading percentages for PPyCQD200 composite (Inset: 3D images of PPyCQD).

Preprints (www.preprints.org) | NOT PEER-REVIEWED | Posted: 15 June 2023 doi:10.20944/preprints202306.1136.v1

3.2. 1D EMW materials

Due to their high anisotropy and multiple scattering effect, one-dimensional (1D) nanofibers have been identified as highly beneficial micromorphology. [21, 51] The high aspect ratio of these fibers supports electron conduction and facilitates efficient loss of conduction. Researchers have shown wide interest in 1D nanomaterials, which comprise nanofibers (NFs),[52] nanowires (NWs),[18] nanochains,[9] and nanotubes (NTs).[53] 1D magnetic nanostructures offer significant advantages, including extending the path of electromagnetic wave transmission and enhancing attenuation effects. Furthermore, a unique double network consisting of a one-dimensional anisotropic magnetic interaction and an interpenetrating conductive network was constructed. The anisotropic magnetic interaction network elongates and interacts with external electromagnetic fields, resulting in attenuated electromagnetic waves. Meanwhile, the conductive network enables the formation of microcurrents and multiple reflections of electromagnetic waves.[54] Additionally, 1D magnetic nanostructures has been proved to modulate the distribution of microelectric fields and thus facilities the effect of electromagnetic polarization. Thus, 1D magnetic nanomaterials have potential applications as microwave absorbers across a wide frequency range.[55]

Regarding the preparation methods of 1D EMW nanoabsorption materials, there are mainly three categories: electrospinning, solvothermal/hydrothermal, and self-assembly methods. Among these, electrospinning is particularly noteworthy due to its flexible operation, low cost, and favorable safety considerations. Furthermore, it is an ideal approach for designing one-dimensional carbon-matrix nanofibers that are modified with metallic or metallic oxide nanoparticles. Qiao fabricated the titanium oxide and metallic cobalt decorated 1D carbon nanofibers (TiO_2/Co/CNFs) by electrospinning method (Figure 4a).[56] The diameter of the TiO_2/Co/CNFs is mainly concentrating on ~ 280 nm, and the surface was randomly distributed of cobalt particle size (average dimeter is 130 nm, respectively). Cross-connected TiO_2/Co/CNFs formed a three-dimensional micro-network structure (Figure 3b-c), and the resulting material demonstrated both tunable and highly efficient electromagnetic absorption capacity. TiO_2/Co/CNFs shows the RL_{min} of -50 dB under 3.5 mm and broad effective absorption bandwidths exceed 5.2 GHz. Among them, n-type TiO_2 presented strong dielectric loss abilities, as well as the magnetic Co nanoparticles offered additional magnetic loss (high Snoek's limit[57] and the suppressed the skin effect[58]).

Prof. Cao reported $CeNiCo_2O_4$ porous nanofiber constructed by electrospinning and *in-situ* heat treatment.[56] As shown in Figure 3d, Co^{2+} and Ni^{2+} ions are reduced to CoNi alloy under thermal treatment,[59] and randomly distributed on the smooth pristine nanofiber. The average diameters of the C-N1-3 fibers are focus on ~200, ~180 and ~170 nm, respectively. All the C-$NiCo_2O_4$ nanofibers exhibit prominent EM absorption abilities. Among them, the RL_{min} of C-N1 reaches -52.7 dB at 15.6 GHz, and that of C-N2 is -51 dB at 8.56 GHz. The possible EM wave attenuation mechanisms are predicted in Figure 4e. Initially, unique three-dimensional micro-network structure consist of the carbon matrix and magnetic nanoparticles presents appropriate conductivity and conductive loss. Secondly, the interfacial polarization arising from the metal oxide/C and magnetic particle/C interface ascribed to the enhanced dielectric loss. Thirdly, metallic magnetic particles introduce magnetic loss, which further enhances absorption capacity. Additionally, the micro-network structure effectively enlarges the multiple scattering effects, which promote the attenuation of electromagnetic waves. All these benefits work together to create a highly efficient and tunable absorption material.

Preprints (www.preprints.org) | NOT PEER-REVIEWED | Posted: 15 June 2023 doi:10.20944/preprints202306.1136.v1

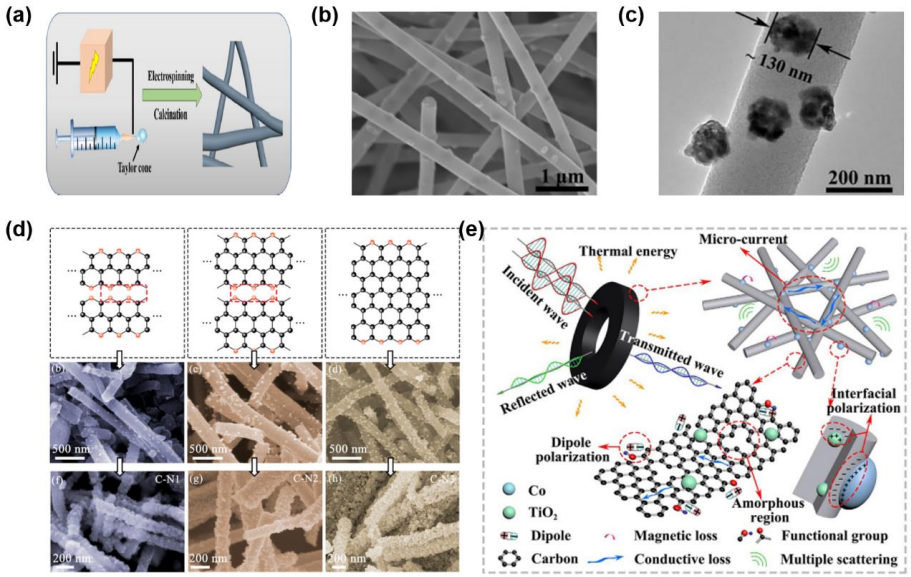

Figure 4. (a) Schematic illustration of electrostatic spinning. (b) FESEM image and (c) HRTEM image of TiO_2/Co/CNFs. (d) SEM images of C-CoNi treated at 500, 600 and 700 °C. (e) EMW loss mechanisms.

Hydrothermal treatment promotes the formation of one-dimensional fibers with high surface-area-to-volume ratios, making them highly suitable for the deposition of active materials onto their surfaces. This method offers several advantages over other synthetic techniques, including its simplicity, low cost, and high uniformity in the distribution of active materials. Prof. Wu reported novel 1D CF@$NiFe_2O_4$ composite coated with phytic acid-doped polyaniline (CF@$NiFe_2O_4$@p-PANI) materials (Figure 5a).[60] The magnetic saturation (Ms) value reached 29.9 emu g^{-1} and depicted a RL_{min} of -46 dB with a thin thickness of 2.9 mm, which may attributed to its ideal matching of magnetic loss and dielectric loss, interfacial polarizations, eddy current loss and interface relaxation. Ma and coauthors prepared high-performance 1D Fe_3O_4@SiO_2@NiO (FSN) nanochains for microwave absorption[61]. As shown in Figure 5d, flower-like NiO nanosheets grows on the Fe_3O_4 nanoparticles surface. Induced by large surfaces, multiple interfaces, and void spaces, the FSN nanochains showed excellent MA properties of -54.28 dB (12.9 GHz) and wide effective absorption bandwidth of 4.0 GHz (11.05-15.05 GHz) at the thickness of 2.54 mm. This work demonstrates that build the unique flower-like and multi-layered yolk-shell structure of 1D flower-like FSN yolk-shell nanochains benefits the microwave/material interactions, adjusting the dielectric properties, offering a promising method for fabricating superior 1D EM absorption materials. Moreover, Ma reported $NiCo_2O_4$ nanosheets decorated on $ZnFe_2O_4$@SiO_2@C nanochains (ZSCNC).[62] Unique 1D flower-like architectures of large surfaces and multiple interfaces (Figure 6g) made 1D ZSCNC nanochains an excellent MA material. ZSCNC nanochains presented outstanding RL_{min} of -54.29 dB (11.14 GHz, Figure 5h) and an EAB of 5.66 GHz (11.94-17.60 GHz) at 2.39 mm. Additionally, 3D RL diagrams (Figure 6i) revealed that ZSCNC nanochains possess much better MA performances than 1D ZSC nanochains.

Preprints (www.preprints.org) | NOT PEER-REVIEWED | Posted: 15 June 2023 doi:10.20944/preprints202306.1136.v1

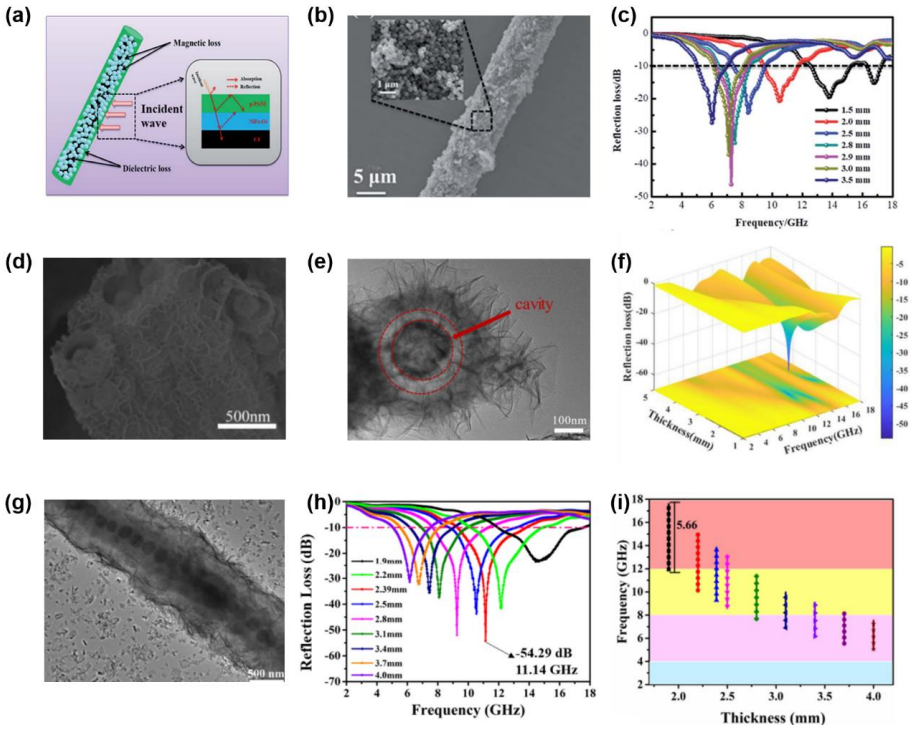

Figure 5. (a) Schematic illustration of the EM absorption mechanism for the CF@$NiFe_2O_4$@p-PANI hybrid. (d) SEM image and (e) TEM image of 1D FSN nanochains. (f) RL curves of the sample loaded with 30 wt% FSN nanochains at different layer thicknesses. (g) TEM images of 1D ZSCNC nanochains. (h) RL curves and (i) EAB of the samples loaded with ZSCNC nanochains with different layer thicknesses.

3.3. 2D EMW materials

Two-dimensional (2D) nanomaterials, including graphene, MXenes, MoS_2 nanosheets, layered double hydroxides (LDHs), graphite-like C_3N_4, and graphene, presents large exposed surfaces, low density, and unique electric behavior,[63-64] and was regarded as potential alternatives for high-performance absorption materials.[14, 65-66]

As a traditional MA material, carbon-based materials such as carbon fibers,[21, 51, 60, 67] carbon nanotubes[68-69] and graphene oxide (GO)[24, 70] are ideal candidates. In recent years, GO has become a highly ideal EM absorber owing to its unique 2D structure and excellent properties of low density, excellent electrical conductivity, lightweight, high specific surface area, high electron mobility, and numerous surface defects.[47-49] Despite these advantages, GO's ultra-high conductivity and dielectric constant do not suffice to meet the requirements of impedance matching, resulting in weak attenuation and strong skin reflection. As a result, extensive research efforts have been directed towards the rational design of GO-based composites, with the goal of achieving exceptional microwave absorption performance.[71-72]

Prof. Che built CeO_{2-x}/RGO hybrid materials with accordion-like structure.[63] The typical TEM image in Figure 6a shows that the 2 nm-size CeO_{2-x} NPs are homogeneous anchored on both sides of RGO sheets. In **Figure 6b**, the 3D-laminated lightweight CeO_{2-x}/RGO composite exhibits excellent attenuation ability of an ultrabroad bandwidth (5.84 GHz) and a maximum reflection loss (-50.6 dB) which depicted to the well impedance matching and synergistic effect between RGO sheets and the embedded CeO_{2-x} NPs. Hierarchical CeO_{2-x}/RGO structure demonstrates a strong dielectric loss by leveraging the polarization and relaxation induced by the defects in RGO, resulting in the efficient modification of the complex permittivity value.[58, 73-74] This is further enhanced by the high density of interfaces together with extended the propagation path of microwaves through multiple scatterings and reflections, achieving even greater microwave attenuation (Figure 6c).[75-76] Furthermore, charge transfers between RGO and CeO_{2-x} heterostructure will attribute to charge accumulation around CeO_{2-x} NPs, caused by the different intrinsic conductivity.[77]

Preprints (www.preprints.org) | NOT PEER-REVIEWED | Posted: 15 June 2023 doi:10.20944/preprints202306.1136.v1

Prof Huang reported strong absorption and broad bandwidth EM absorption materials of hierarchically Ni-doped Fe_3O_4@C/rGO aerogels.[7] Free Fe^{3+} prevent the restacking of GO nanosheets via metal-oxygen covalent or electrostatic interactions. As revealed in Figure 6d, Ni-doped Fe_3O_4@C/rGO aerogel show a 3D interconnected porous microstructure with numerous Fe_3O_4 NPs on rGO surfaces. The enlarged SEM and TEM images further confirm the core-shell structure (inset of Figure 7d). Ni-doped Fe_3O_4@C/rGO presents notable EM absorption performance of strong absorption (- 58.1 dB and 6.48 GHz) and broad bandwidth (- 46.2 dB and 7.92 GHz) with ultralow filling contents of 0.7 and 0.6 wt%, respectively. CST simulation results in Figure 6e illustrates weak scattering signals at 10 and 15 GHz, which is ascribed to the synergistic effects of unique hierarchically porous structures and heterointerface engineering. Achieving high RL, thin thickness, and light weight simultaneously is still a significant challenge for graphene-based MA, which limited by the inherent impedance matching and attenuation ability. Ma reported ultrathin and light-weight Fe_3O_4@C/GA materials with precisely tunable density.[78] Fe_3O_4@C microspheres were anchored on the surface of GA network by using APTES as a surface modifier and a cross-linker, presents a superlight density of 4.95 mg·cm^{-3} (Figure 6g). Superior Fe_3O_4@C/GA delivered an unprecedented RL_{min} of -54.0 dB and 80% of the K-band was covered at a thickness less than 1 mm. This result may be attributed to the strong interfacial polarization and impedance matching induced by Fe_3O_4, as well as the increased dielectric loss tangent and appropriate permeability.

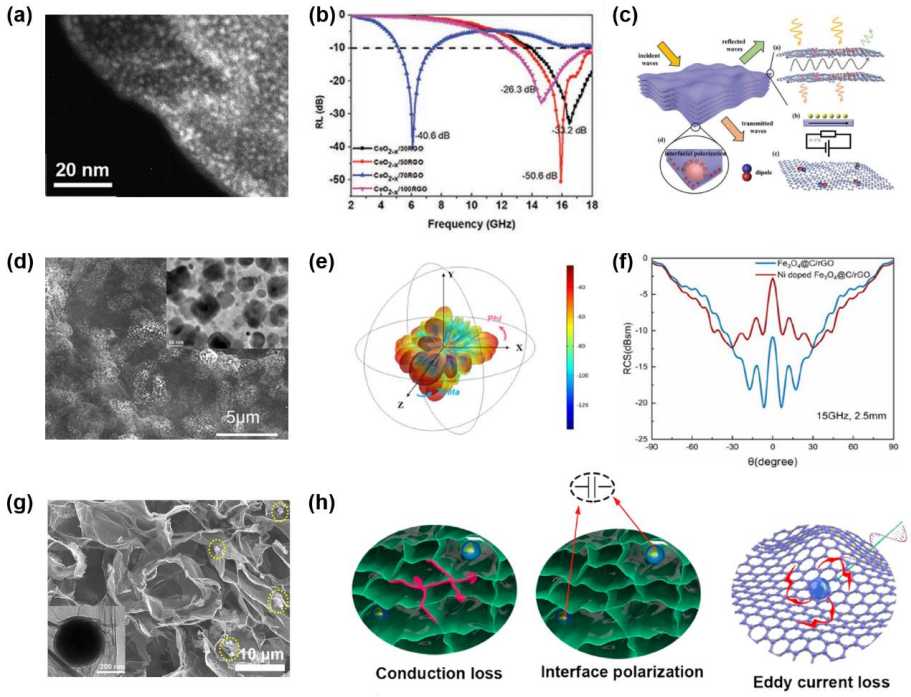

Figure 6. (a) The HAADF images of accordion-like CeO_{2-x}/RGO composites. (b) The RL_{min}, (c) The EM absorption mechanisms of CeO_{2-x}/RGO absorbers. (d) SEM images of the Ni-doped Fe_3O_4@C/rGO aerogel. (e) 3D radar wave scattering signals and (f) RCS simulated curves of Ni-doped Fe_3O_4@C/rGO aerogels. (g) SEM image (inset: TEM image) of the Fe_3O_4@C/GA50 composite. (h) Schematic illustration of EM absorption mechanisms in GA and composite.

MXene is a novel 2D nanomaterial own the merits of hydrophilicity, tunable electrical conductivity, and abundant surface functional groups (OH, O, and/or F groups).[2, 64] The high electrical conductivity makes MXene more productive than graphene in constructing conductive network and strong conduction loss. Abundant functional groups lead to dipole and interfacial polarization, contributing to considerable polarization loss.[27, 79-80] Furthermore, the flexible 2D structure of MXene with large aspect ratio allows the fabrication of porous macroscopic scale assemblies[19] and also makes it an ideal nanosubstrate for hybridization for balancing the loss capacity and the impedance behavior, which can further improve MA performance.[81-82] Most of the reported MXene-related

Preprints (www.preprints.org) | NOT PEER-REVIEWED | Posted: 15 June 2023 doi:10.20944/preprints202306.1136.v1

MA studies are based on the use of multi-layered $Ti_3C_2T_x$. Qing reported the investigation of the $Ti_3C_2T_x$ MXene.[83] Multi-layered $Ti_3C_2T_x$ nanosheets showed higher relative complex permittivity and MA intensity, and reaches a broad frequency range of 12.4–18 GHz with exceeded −11 dB. However, low absorption intensity limited its development.

Recently, Prof. Lu reported hollow Fe_3O_4 nanoparticles (HFO) MXene-hollow Fe_3O_4 nanoparticles (HFO) hybrids to pursue the light weight and strong absorption ability (Figure 7b).[84] As shown in Figure 7, the MXene/HFO hybrids achieved a high EM wave absorption performance of -63.7 dB at a thin thickness of 1.56 mm, which may be caused by the synergistic effect of dielectric loss, magnetic loss, interface polarization and improved impedance matching. Cui reported 3D porous MXene/Ni composite microspheres as high effective EM absorb materials.[85] In Figure 7d, homogeneous Ni nanochains and $Ti_3C_2T_x$ nanosheets suspension were drop into liquid paraffin, causing the unique 3D porous interconnection network, which benefit to release the stacking of $Ti_3C_2T_x$ nanosheets and the agglomeration of magnetic Ni nanochains. Emerged hetero-interface and abundant function surface groups provide MXene/Ni composite microspheres with good impedance matching and excellent EMW absorption performance (RL_{min} is -52.7 dB@12.8 GHz at 1.9 mm).

Moreover, Prof. Lu reported N-doped MXene/hollow Co-ZIF (Ti_3CNT_x/HCF) hybrids as MA materials.[86] The hollow HCF particles with the average diameter about 500-600 nm were evenly dispersed on the surface of Ti_3CNT_x (Figure 7e), generating abundant heterointerfaces. Accompanied with the improved impedance matching, Ti_3CNT_x/HCF achieved strong EMW absorption ability (reflection loss of -55.02 dB, Figure 7f) with low filler loading. Chen reported CoFe-MOF@$Ti_3C_2T_x$ composites materials towards broadband microwave absorption (Figure 7g-i).[87] Core-shell structure Co/CNTs-MXene@CF shows boosted electron transfer paths, and realize appropriate conductivity and abundant heterointerfaces, which may accelerate the conduction loss and interfacial polarization response. As expected, Co/CNTs-MXene@CF heterostructures exhibit the strong reflection loss of -61.41 dB at 2.52 mm and achieve broad effective absorption bandwidth reaches of 5.04 GHz. These results demonstrate that the optimized magnetic particle anchored on 2D functional framework will dramatically improves the electromagnetic wave attenuation ability.

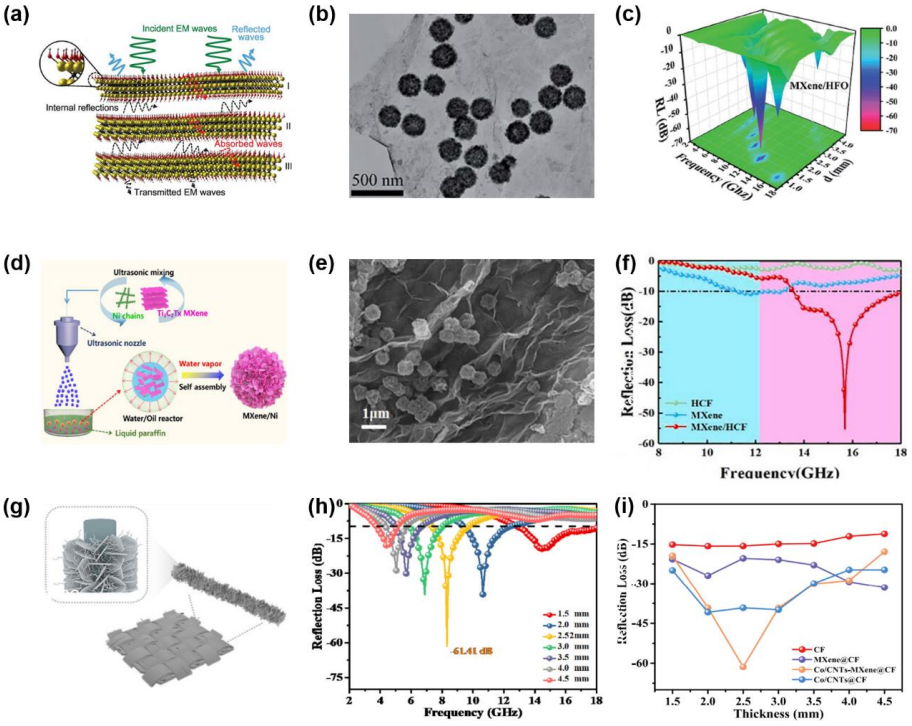

Figure 7. (a) Proposed EM absorption mechanism of MXene. (b) The TEM images of MXene/HFO hybrids. (c) The 3D RL maps of MXene/HFO hybrids. (d) Synthesis and formation mechanism of MXene/Ni. (e) The SEM images and (f) 3D RL of the Ti_3CNT_x/HCF hybrids samples. (g) Schematic illustration of the synthetic process of Co/CNTs-MXene@CF. RL value of (h) Co/CNTs-MXene@CF and (i) corresponds to different thickness.

Preprints (www.preprints.org) | NOT PEER-REVIEWED | Posted: 15 June 2023 doi:10.20944/preprints202306.1136.v1

Recently, multicomponent dielectric/magnetic micro/nanounits with microscopic 3D porous, hollow, core-shell, yolk-shell, or core-sheath structures have been developed as effective EMA materials. The dielectric/ magnetic components and the hierarchical microstructures endow the micro/nanounits with excellent impedance matching and synergetic electromagnetic losses.[88] Prof. Yin reported the RGO/$Ti_3C_2T_x$ core-shell heterostructure to realize ultrahigh EM absorption performance.[89] Figure 8a clearly shows the morphologies of the RGO/$Ti_3C_2T_x$ composites. Large size RGO flakes entirely wrapped the $Ti_3C_2T_x$ spheres and connect the adjacent to form a porous network. It's worth noting that as the $Ti_3C_2T_x$ spheres content increases, the matching thickness decreases to a remarkable 3.2 mm, where the EAB covering the entire X-band and displaying a density of approximately 0.0033 mg cm^{-3}, as shown in Figure 10b. Notably, with an increase in sample thickness, the strongest absorption peaks exhibit a gradual shift towards lower frequencies, indicating remarkable absorption performance even at lower frequencies, as displayed in Figure 10c.

Shui reported a $Ti_3C_2T_x$ MXene sponge foam (MSF) through facile dip-coating method.[90] MSF maintains the intrinsically lightweight feature with low mass loading of $Ti_3C_2T_x$ (less than 22.5%, Figure 8d). Depicted from the macroscopic impedance matching to free space and various microscopic morphologies, the obtained MSF presents high THz absorption over 99.99% under the 100% qualified frequency bandwidth ranging from 0.3 to 1.65 THz (Figure 10e). The superior absorption mechanism is summarized in Figure 10f. The incident THz wave is coming will totally enter the MSF composite due to the open structure with a large aperture. Less than 0.06% (MSF with 2 mm thickness) EM wave will be reflected to the air. Moreover, the THz wave would be attenuated by multiply reflected by $Ti_3C_2T_x$, inside the MSF caused by a long transmission path.[91-92] Liang designed 3D dielectric $Ti_3C_2T_x$/RGO aerogel anchored with magnetic Ni nanochains composite materials.[39] Ni/MXene/GO (NiMG) aerogel demonstrates anisotropic cellular structure with the assistance of unidirectional ice template. Interestingly, ultralight NiMR-H delivers the best EMA performance of -75.2 dB together with a broadest EAB of 7.3 GHz, which exceed 99.999996% EM wave was absorbed. Unique cell structure and dielectric/magnetic hetero-interfaces benefit to reach perfect impedance matching, multiple polarizations, and electric/magnetic-coupling effects.

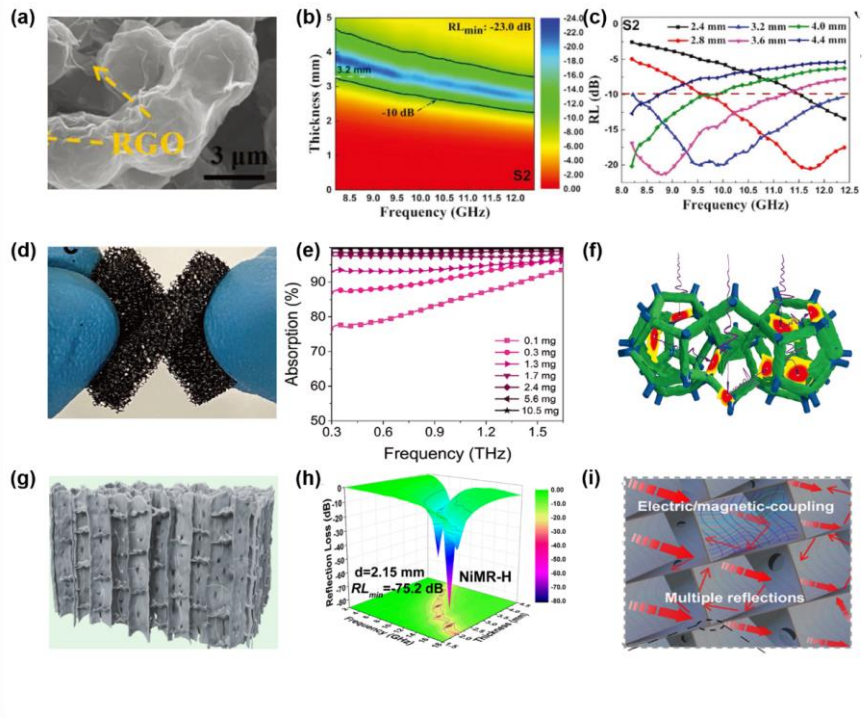

Figure 8. (a) SEM images of hollow RGO/$Ti_3C_2T_x$ foam. (b) The 2D contours of *RL* values and (c) The *RL* value versus frequency and thickness of S2. (d) Digital images of MSF with twisting. (e) THz absorption by MSF with different filling amounts of $Ti_3C_2T_x$ flakes. (f) The THz absorption mechanism of MSF. (g) Schematic illustration of NiMR-H aerogel. (h) 3D RL curves of NiMR-H aerogels. (i) schematic illustrations of the EMA mechanism.

Preprints (www.preprints.org) | NOT PEER-REVIEWED | Posted: 15 June 2023 doi:10.20944/preprints202306.1136.v1

Prof. Lu fabricated the 2D/1D/0D $Ti_3C_2T_x$/carbon nanotubes/Co nanocomposite via an electrostatic assembly.[65] As shown in Figure 9a, the porous CNTs/Co nanocomposites uniformly anchored on the surface of sheet-like $Ti_3C_2T_x$, in which 0D Co nanoparticles were well-dispersed inside the carbon spheres. Surprisingly, a strong reflection loss of -85.8 dB and an ultrathin thickness of 1.4 mm were achieved. The excellent EM wave absorption can be attributed to the fast charge carriers, electric/magnetic dipole polarization, interfacial polarization, natural resonance, and multiple internal reflections (Figure 9b). Figure 10c demonstrates the frequency-dependent attenuation constant α. The order of α value was CNTs/Co< $Ti_3C_2T_x$ /CNTs/Co< $Ti_3C_2T_x$. However, $Ti_3C_2T_x$ presents limited impedance matching. Thus, the combination of attenuation ability and promoted impedance matching contributed to outstanding microwave absorbing performances in the laminated $Ti_3C_2T_x$/ CNTs/Co nanocomposites.

Currently, diverse transition metal sulfides have been demonstrated as functional EMW absorbers owning to their remarkable RL.[93-94] Man reported elaborate yolk-shell FeS_2@C nanocomposite as EMW absorption materials.[95] Yolk-shell FeS_2@C nanospindles was synthesized via a facile coating-carbonation-sulfidation strategy, as shown in Figure 9d. FeS_2@C delivers strong RL of -45 dB and a broad 15.4 GHz bandwidth, caused by the significant cavity and interfacial effects (Figure 9e). Prof. Cao reported coaxial stacking VS_2 nanosheets (CSVNs) with absorption in multiple bands and strong absorption performance (Figure 10f).[96] The VS_2 nanosheets exhibited unique dual-band absorption characteristics in the C-band and Ku-band. A RL_{min} of -57 dB were obtained. Prof. Cao find that NbS_2 possesses good conductivity and abundant active sites, which regarded as excellent EM absorption materials.[97] The wall thicknesses of NbS_2 nanospheres is ~126 nm, the frequency bands are tunable from the C-band to the X-band, and even the Ku-band through reducing the wall thickness of NbS_2. In Figure 10h, NbS_2 nanospheres delivers a RL_{min} of -43.85 dB with a wide bandwidth of 6.48 GHz. The predicted absorption mechanisms of NbS_2 are depicted in **Figure 10i**. Abundant electrochemical active sites, multiphase structure, and high conductivity endow NbS_2 to realize excellent EMW absorption performance, where the 1T/2H interfaces facilitate the dipole polarization, and the mixture of metallic and semiconductive phases enhance the electron transfer.[98-99] The multiple interlaced NbS_2 nanosheets also provide diverse attenuation pathways, and promote the electron hopping between adjacent NbS_2 nanosheets.[97, 100]

Preprints (www.preprints.org) | NOT PEER-REVIEWED | Posted: 15 June 2023 doi:10.20944/preprints202306.1136.v1

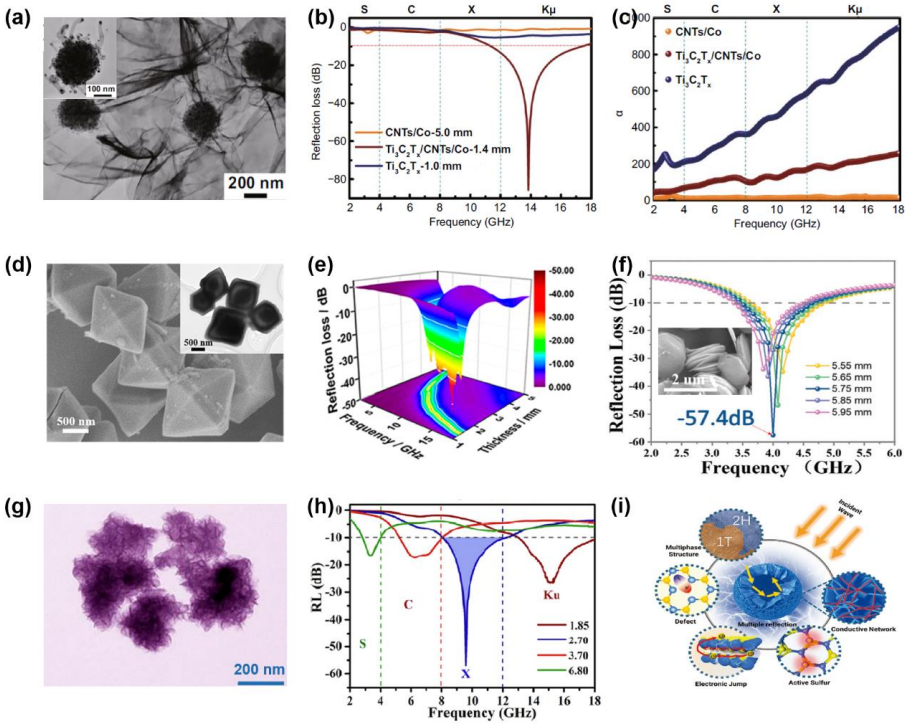

Figure 9. (a) TEM images of $Ti_3C_2T_x$/CNTs/Co (inset: TEM images of CNTs/Co). (b) The *RL* curves and (c) The α of CNTs/Co-5.0 mm, $Ti_3C_2T_x$/CNTs/Co-1.4 mm, and $Ti_3C_2T_x$-1.0 mm. (d) FESEM image of FeS_2@C (inset: TEM image of FeS_2@C). (e) 3D RL values of FeS_2@C with 55 wt % filler loading. (f) RL value at 4 GHz for sample S-190 with a thickness of 5.55-5.95 mm (inset: SEM images of the S-190 samples). (g) SEM images of S24. (h) The RL curves aim at specific frequency band of S24. (i) Schematic illustration of the of EMW absorption mechanisms for NbS_2.

4. Perspectives

As previously mentioned, electromagnetic absorbing materials can be designed to meet the requirements of "thinner thickness, lighter weight, wider frequency band, and higher absorption strength." We believe that EM functions and devices offer enormous potential for development. Moreover, there are three primary directions for future research: 1) Synthesis and manufacturing of hierarchical LD EM functional materials, such as a combination of 0D nanocrystals, 1D nanotubes/nanowires/nanorods, and 2D nanosheets. This approach is likely to bring about innovative breakthroughs in EM functions and devices. The developed materials not only inherit the characteristics of the basic units but also produce coupling/synergistic effects when these units combine, resulting in high or even ultra-performance. 2) Regulating crystal and electronic structures. Tunning the crystal and electronic structures, band structures, the density of states, and charge distributions will help us understand the electromagnetic response and energy conversion mechanisms. We can integrate scientific calculations, reference models, and formulas is important to facilitate exploring more low-dimensional EM functional materials. 3) Smart wearable field. Intelligent absorbing materials can make corresponding responses based on signals and adapt to temperature, humidity, electromagnetic wave strength changes, etc. These materials achieve self-diagnosis, self-adaptation, and self-repairing abilities, making them valuable for wearable EM protection, military stealth, and other fields.

5. Conclusions

Low-dimensional materials have regarded as important materials for EMW wave absorption, since the excellent EMW loss ability originated from the unique electronic structures and large surface areas. As a result, Low-dimensional materials have recently reached remarkable achievements. Better

performance will be obtained by reasonably designing the elaborate structures and optimizing the multi-components. Nevertheless, the fundamental structure-function relationship is remains challenging. Balancing the regulation of crystal structure, heterointerface and morphology will facilitate the prediction and regulation of EMW absorption performance. Despite boosting the intensity, such as scaleup ability, stability and repeatability are expected to be imperative in the future.

Author Contributions: writing-original draft preparation, H.X. and T.T.; writing-review and editing, Z.M., X. W., H.Z. and H.X.; supervision, C. L. H.X. and T.T. contribute equally in this manuscript. All authors have read and agreed to the published version of the manuscript.

Funding: This research was funded by the Science Foundation of Zhejiang Sci-Tech University (Grants 22212127-Y), the National Natural Science Foundation of China (Grants 52101218, 22271254) and the Zhejiang Provincial Natural Science Foundation of China (Grants LQ22E010004).

Conflicts of Interest: The authors declare no conflict of interest.

References

1. Cao, M. S.; Wang, X. X.; Zhang, M.; Shu, J. C.; Cao, W. Q.; Yang, H. J.; Fang, X. Y.; Yuan, J., Electromagnetic Response and Energy Conversion for Functions and Devices in Low-Dimensional Materials. *Adv. Funct. Mater.* **2019,** *29*, 1807398.
2. Faisal S.; Mohamed A.; Christine B. H.; Babak.; Soon M.; Chong M. K.; Yury G., Electromagnetic interference shielding with 2D transition metal carbides (MXenes). *Science* **2016,** *353*, 1137-1140.
3. Aamir I.; Faisal S.; Kanit H.; Myung-Ki K.; Jisung K.; Junpyo H.; Hyerim K.; Daesin K.; Yury G.; Chong M. K., Anomalous absorption of electromagnetic waves by 2D transition metal carbonitride Ti_3CNT_x (MXene). *Science* **2020,** *369*, 446–450.
4. Balci, O.; Polat, E. O.; Kakenov, N.; Kocabas, C., Graphene-enabled electrically switchable radar-absorbing surfaces. *Nat. Commun.* **2015,** *6*, 6628.
5. Hong, S. K.; Kim, K. Y.; Kim, T. Y.; Kim, J. H.; Park, S. W.; Kim, J. H.; Cho, B. J., Electromagnetic Interference Shielding Effectiveness of Monolayer Graphene. *Nanotechnology* **2012,** *23*, 455704.
6. Yang, B.; Fang, J.; Xu, C.; Cao, H.; Zhang, R.; Zhao, B.; Huang, M.; Wang, X.; Lv, H.; Che, R., One-Dimensional Magnetic FeCoNi Alloy Toward Low-Frequency Electromagnetic Wave Absorption. *Nanomicro. Lett.* **2022,** *14*, 170.
7. Huang, X.; Wei, J.; Zhang, Y.; Qian, B.; Jia, Q.; Liu, J.; Zhao, X.; Shao, G., Ultralight Magnetic and Dielectric Aerogels Achieved by Metal-Organic Framework Initiated Gelation of Graphene Oxide for Enhanced Microwave Absorption. *Nanomicro. Lett.* **2022,** *14*, 107.
8. Borchers, A.; Pieler, T., Programming pluripotent precursor cells derived from Xenopus embryos to generate specific tissues and organs. *Nanomaterials* **2010,** *1*, 413-26.
9. You, W.; Pei, K.; Yang, L.; Li, X.; Shi, X.; Yu, X.; Guo, H.; Che, R., In situ dynamics response mechanism of the tunable length-diameter ratio nanochains for excellent microwave absorber. *Nano Res.* **2019,** *13*, 72-78.
10. Hashemi, S. A.; Ghaffarkhah, A.; Hosseini, E.; Bahrani, S.; Najmi, P.; Omidifar, N.; Mousavi, S. M.; Amini, M.; Ghaedi, M.; Ramakrishna, S.; Arjmand, M., Recent progress on hybrid fibrous electromagnetic shields: Key protectors of living species against electromagnetic radiation. *Matter* **2022,** *5*, 3807-3868.
11. Jia, Z.; Zhang, M.; Liu, B.; Wang, F.; Wei, G.; Su, Z., Graphene Foams for Electromagnetic Interference Shielding: A Review. ACS Appl. Nano Mater. **2020,** 3 (7), 6140-6155.
12. Su, X.; Liu, Y.; Liao, Z.; Bi, Y.; Chen, Y.; Ma, Y.; Chung, K. L.; Wan, F.; Ma, M., A review of 1D magnetic nanomaterials in microwave absorption. *J Mater Sci* **2023,** *58*, 636-663.
13. Cao, W. Q.; Wang, X. X.; Yuan, J.; Wang, W. Z.; Cao, M. S., Temperature Dependent Microwave Absorption of Ultrathin Graphene Composites. *J. Mater. Chem. C* **2015,** *3*, 10017-10022.
14. Zhang, S.; Cheng, B.; Gao, Z.; Lan, D.; Zhao, Z.; Wei, F.; Zhu, Q.; Lu, X.; Wu, G., Two-Dimensional Nanomaterials for High-Efficiency Electromagnetic Wave Absorption: An Overview of Recent Advances and Prospects. *J. Alloys Compounds* **2022,** *893*, 162343.
15. Jiang, Y.; Fu, X.; Zhang, Z.; Du, W.; Xie, P.; Cheng, C.; Fan, R., Enhanced Microwave Absorption Properties of Fe_3C/C Nanofibers Prepared by Electrospinning. *J. Alloys Compounds* **2019,** *804*, 305-313.

16. Voiry, D.; Shin, H. S.; Loh, K. P.; Chhowalla, M., Low-Dimensional Catalysts for Hydrogen Evolution and CO_2 Reduction. *Nat. Rev. Chem.* **2018,** *2*, 0105.
17. Bi, Y.; Ma, M.; Liao, Z.; Tong, Z.; Chen, Y.; Wang, R.; Ma, Y.; Wu, G., One-dimensional Ni@Co/C@PPy Composites for Superior Electromagnetic Wave Absorption. *J. Colloid Interface Sci.* **2022,** *605*, 483-492.
18. Han, X.; Huang, Y.; Wang, J.; Zhang, G.; Li, T.; Liu, P., Flexible Hierarchical ZnO/AgNWs/Carbon Cloth-based Film for Efficient Microwave Absorption, High Thermal Conductivity and Strong Electro-thermal Effect. *Composites Part B: Engineering* **2022,** *229*, 109458.
19. Cao, M. S.; Cai, Y. Z.; He, P.; Shu, J. C.; Cao, W.-Q.; Yuan, J., 2D MXenes: Electromagnetic Property for Microwave Absorption and Electromagnetic Interference Shielding. *Chem. Eng. J.* **2019,** *359*, 1265-1302.
20. Zhang, X.; Dong, Y.; Pan, F.; Xiang, Z.; Zhu, X.; Lu, W., Electrostatic Self-Assembly Construction of 2D MoS_2 Wrapped Hollow Fe_3O_4 Nanoflowers@1D Carbon Tube Hybrids for Self-Cleaning High-Performance Microwave Absorbers. *Carbon* **2021,** *177*, 332-343.
21. Wang, F.; Sun, Y.; Li, D.; Zhong, B.; Wu, Z.; Zuo, S.; Yan, D.; Zhuo, R.; Feng, J.; Yan, P., Microwave Absorption Properties of 3D Cross-Linked Fe/C Porous Nanofibers Prepared by Electrospinning. *Carbon* **2018,** *134*, 264-273.
22. Huo, J.; Wang, L.; Yu, H., Polymeric Nanocomposites for Electromagnetic Wave Absorption. *J. Mater. Sci.* **2009,** *44*, 3917-3927.
23. Liao, J.; Ye, M.; Han, A.; Guo, J.; Liu, Q.; Yu, G., Boosted Electromagnetic Wave Absorption Performance from Multiple Loss Mechanisms in Flower-like Cu_9S_5/RGO Composites. *Carbon* **2021,** *177*, 115-127.
24. Dreyer, D. R.; Ruoff, R. S.; Bielawski, C. W., From Conception to Realization: an Historial Account of Graphene and some Perspectives for its Future. *Angew. Chem. Int. Ed.* **2010,** *49*, 9336-44.
25. Xia, Y.; Gao, W.; Gao, C., A Review on Graphene-Based Electromagnetic Functional Materials: Electromagnetic Wave Shielding and Absorption. *Adv. Funct. Mater.* **2022,** *3*, 2204591.
26. Wang, M.; Fang, P. F.; Chen, Y.; Leng, X. Y.; Yan, Y.; Yang, S. B.; Xu, P.; Yan, C., Synthesis of Highly Stable LTO/rGO/SnO_2 Nanocomposite via In Situ Electrostatic Self-Assembly for High-performance Lithium-Ion Batteries. *Adv. Funct. Mater.* **2023,** 221390.
27. Song, Q.; Ye, F.; Kong, L.; Shen, Q.; Han, L.; Feng, L.; Yu, G.; Pan, Y.; Li, H., Graphene and MXene Nanomaterials: Toward High-Performance Electromagnetic Wave Absorption in Gigahertz Band Range. *Adv. Funct. Mater.* **2020,** *30*, 2000475.
28. Wen, B.; Cao, M. S.; Hou, Z. L.; Song, W. L.; Zhang, L.; Lu, M. M.; Jin, H. B.; Fang, X. Y.; Wang, W. Z.; Yuan, J., Temperature Dependent Microwave Attenuation Behavior for Carbon-Nanotube/Silica composites. *Carbon* **2013,** *65*, 124-139.
29. Cao, M.; Wang, X.; Cao, W.; Fang, X.; Wen, B.; Yuan, J., Thermally Driven Transport and Relaxation Switching Self-Powered Electromagnetic Energy Conversion. *Small* **2018**, e1800987.
30. Song, W. L.; Cao, M. S.; Hou, Z. L.; Fang, X. Y.; Shi, X. L.; Yuan, J., High Dielectric Loss and its Monotonic Dependence of Conducting-Dominated Multiwalled Carbon Nanotubes/Silica Nanocomposite on Temperature Ranging from 373 to 873 K in X-band. *Appl. Phys. Lett.* **2009,** *94*, 233110.
31. Wen, B.; Cao, M.; Lu, M.; Cao, W.; Shi, H.; Liu, J.; Wang, X.; Jin, H.; Fang, X.; Wang, W.; Yuan, J., Reduced Graphene Oxides: Light-Weight and High-Efficiency Electromagnetic Interference Shielding at Elevated Temperatures. *Adv. Mater.* **2014,** *26*, 3484-3489.
32. Shu, J. C.; Cao, W. Q.; Cao, M. S., Diverse Metal–Organic Framework Architectures for Electromagnetic Absorbers and Shielding. *Adv. Funct. Mater.* **2021,** *31*, 2100470.
33. Liu, J.; Zhang, L.; Zang, D.; Wu, H., A Competitive Reaction Strategy toward Binary Metal Sulfides for Tailoring Electromagnetic Wave Absorption. *Adv. Funct. Mater.* **2021,** *31*, 2105018.
34. Qin, M.; Zhang, L.; Zhao, X.; Wu, H., Defect Induced Polarization Loss in Multi-Shelled Spinel Hollow Spheres for Electromagnetic Wave Absorption Application. *Adv. Sci.* **2021,** *8*, 2004640.
35. Wang, X. X.; Ma, T.; Shu, J. C.; Cao, M. S., Confinedly Tailoring Fe_3O_4 Clusters-NG to Tune Electromagnetic Parameters and Microwave Absorption with Broadened Bandwidth. *Chem. Eng. J.* **2018,** *332*, 321-330.
36. Wu, Z.; Cheng, H. W.; Jin, C.; Yang, B.; Xu, C.; Pei, K.; Zhang, H.; Yang, Z.; Che, R., Dimensional Design and Core-Shell Engineering of Nanomaterials for Electromagnetic Wave Absorption. *Adv. Mater.* **2022,** *34*, e2107538.
37. Liang, L.; Gu, W.; Wu, Y.; Zhang, B.; Wang, G.; Yang, Y.; Ji, G., Heterointerface Engineering in Electromagnetic Absorbers: New Insights and Opportunities. *Adv. Mater.* **2022,** *34*, e2106195.
38. Zhang, Y.; Wang, X.; Cao, M., Confinedly Implanted $NiFe_2O_4$-rGO: Cluster Tailoring and Highly Tunable Electromagnetic Properties for Selective-Frequency Microwave Absorption. *Nano Res.* **2018,** *11*, 1426-1436.

39. Liang, L.; Li, Q.; Yan, X.; Feng, Y.; Wang, Y.; Zhang, H. B.; Zhou, X.; Liu, C.; Shen, C.; Xie, X., Multifunctional Magnetic $Ti_3C_2T_x$ MXene/Graphene Aerogel with Superior Electromagnetic Wave Absorption Performance. *ACS Nano* **2021,** *15*, 6622-6632.
40. Zhang, Y. R.; Wang, B. C.; Gao, S. L.; Qiu, L. P.; Zheng, Q. H.; Cheng, G. T.; Han, W. P.; Ramakrishna, S.; Long, Y. Z., Electrospun MXene Nanosheet/Polymer Composites for Electromagnetic Shielding and Microwave Absorption: A Review. *ACS Appl. Nano Mater.* **2022,** *5*, 12320-12342.
41. Wang, X. X.; Zhang, M.; Shu, J. C.; Wen, B.; Cao, W. Q.; Cao, M. S., Thermally-Tailoring Dielectric "Genes" in Graphene-based Heterostructure to Manipulate Electromagnetic Response. *Carbon* **2021,** *184*, 136-145.
42. Wang, C.; Murugadoss, V.; Kong, J.; He, Z.; Mai, X.; Shao, Q.; Chen, Y.; Guo, L.; Liu, C.; Angaiah, S.; Guo, Z., Overview of Carbon Nanostructures and Nanocomposites for Electromagnetic Wave Shielding. *Carbon* **2018,** *140*, 696-733.
43. Yang, J.; Liang, Y.; Li, K.; Yang, G.; Yin, S., One-Step Low-Temperature Synthesis of 0D CeO_2 Quantum Dots/2D BiO_X (X = Cl, Br) Nanoplates Heterojunctions for Highly Boosting Photo-Oxidation and Reduction Ability. *Appl. Cat. B: Environ.* **2019,** *250*, 17-30.
44. Moharana, S.; Mahaling, R. N., Green Synthetic Route of Carbon Quantum Dot-Reinforced Graphene Oxide-Poly(Vinylidene Fluoride-Co-Hexa Fluoropropylene) Nanocomposites: Toward High Dielectric Constant and Suppressed Loss. *J. Appl. Poly. Sci.* **2019,** *136*, 47850.
45. Gao, Z.; Xu, B.; Ma, M.; Feng, A.; Zhang, Y.; Liu, X.; Jia, Z.; Wu, G., Electrostatic Self-Assembly Synthesis of $ZnFe_2O_4$ Quantum Dots ($ZnFe_2O_4$@C) and Electromagnetic Microwave Absorption. *Composites Part B: Engineering* **2019,** *179*, 107417.
46. Li, J.; Ma, J.; Chen, S.; Huang, Y.; He, J., Adsorption of Lysozyme by Alginate/Graphene Oxide Composite Beads with Enhanced Stability and Mechanical Property. *Mater. Sci. Eng. C Mater. Biol. Appl.* **2018,** *89*, 25-32.
47. Lv, H.; Yang, Z.; Wang, P. L.; Ji, G.; Song, J.; Zheng, L.; Zeng, H.; Xu, Z. J., A Voltage-Boosting Strategy Enabling a Low-Frequency, Flexible Electromagnetic Wave Absorption Device. *Adv. Mater.* **2018,** *30*, e1706343.
48. Salonitis, K.; Pandremenos, J.; Paralikas, J.; Chryssolouris, G., Multifunctional Materials: Engineering Applications and Processing Challenges. *Int. J. Adv. Manufact. Tech.* **2009,** *49*, 803-826.
49. Narayana, K. J.; Gupta Burela, R., A Review of Recent Research on Multifunctional Composite Materials and Structures with Their Applications. *Mater. Today: Proc.* **2018,** *5*, 5580-5590.
50. Rahal, M.; Atassi, Y.; Ali, N. N.; Alghoraibi, I., Novel Microwave Absorbers Based on Polypyrrole and Carbon Quantum Dots. *Mater. Chem. Phys.* **2020,** *255*, 123491.
51. Wei, Y.; Zhang, L.; Gong, C.; Liu, S.; Zhang, M.; Shi, Y.; Zhang, J., Fabrication of Tin/Carbon Nanofibers by Electrospinning and Their Electromagnetic Wave Absorption Properties. *J. Alloys. Compounds* **2018,** *735*, 1488-1493.
52. Bhaumik, M.; Maity, A.; Mahule, T. S.; Srinivasu, V. V., Low Field Microwave Absorption in Iron Nanoparticles Embedded Polyaniline Nanofibers Composite. *Synth. Metals* **2019,** *249*, 63-68.
53. Ghasemi, A.; Reza Gordani, G.; Ghasemi, E., Co_2W Hexaferrite Nanoparticles-Carbon Nanotube Microwave Absorbing Nanocomposite. *J. Magn. Magn. Mater.* **2019,** *469*, 391-397.
54. Peng, K.; Wang, R.; Chen, H.; Li, S.; Huang, F.; Wang, B.; Zhang, H., Prussian Blue Derived Fe/C Anchoring on Multiwalled Carbon Nanotubes Forming Chain-Like Efficient Electromagnetic Wave Absorbent. *J. Electron. Mater.* **2020,** *49*, 6631-6642.
55. Yusuf, J. Y.; Soleimani, H.; Noorhana, y.; Sanusi, Y. K.; Adebayo, L. L.; Sikiru, S.; Wahaab, F. A., Recent Advances and Prospect of Cobalt Based Microwave Absorbing Materials. *Ceram. Int.* **2020,** *46*, 26466-26485.
56. Han, C.; Zhang, M.; Cao, W. Q.; Cao, M. S., Electrospinning and In-Situ Hierarchical Thermal Treatment to Tailor C-$NiCo_2O_4$ Nanofibers for Tunable Microwave Absorption. *Carbon* **2021,** *171*, 953-962.
57. Wang, Z.; Bi, H.; Wang, P.; Wang, M.; Liu, Z.; Shen, L.; Liu, X., Magnetic and Microwave Absorption Properties of Self-Assemblies Composed of Core-Shell Cobalt-Cobalt Oxide Nanocrystals. *Phys. Chem. Chem. Phys.* **2015,** *17*, 3796-801.
58. Yang, Z.; Lv, H.; Wu, R., Rational Construction of Graphene Oxide with Mof-Derived Porous NiFe@C Nanocubes for High-Performance Microwave Attenuation. *Nano Res.* **2016,** *9*, 3671-3682.
59. Yan, L.; Zhang, M.; Zhao, S.; Sun, T.; Zhang, B.; Cao, M.; Qin, Y., Wire-in-Tube ZnO@Carbon by Molecular Layer Deposition: Accurately Tunable Electromagnetic Parameters and Remarkable Microwave Absorption. *Chem. Eng. J.* **2020,** *382*, 122860.

60. Feng, A.; Ma, M.; Jia, Z.; Zhang, M.; Wu, G., Fabrication of $NiFe_2O_4$@Carbon Fiber Coated with Phytic Acid-Doped Polyaniline Composite and Its Application as an Electromagnetic Wave Absorber. *RSC Adv.* **2019,** *9*, 25932-25941.
61. Ma, M.; Li, W.; Tong, Z.; Huang, W.; Wang, R.; Lyu, P.; Ma, Y.; Wu, G.; Yan, Q.; Li, P.; Yao, X., Facile Synthesis of the One-Dimensional Flower-Like Yolk-Shell Fe_3O_4@SiO_2@NiO Nanochains Composites for High-Performance Microwave Absorption. *J. Alloys Compounds* **2020,** *843*, 155199.
62. Ma, M.; Li, W.; Tong, Z.; Ma, Y.; Bi, Y.; Liao, Z.; Zhou, J.; Wu, G.; Li, M.; Yue, J.; Song, X.; Zhang, X., $NiCo_2O_4$ Nanosheets Decorated on One-Dimensional $ZnFe_2O_4$@SiO_2@C Nanochains with High-Performance Microwave Absorption. *J Colloid Interface Sci,* **2020,** *578*, 58-68.
63. Li, Q.; Zhao, Y.; Li, X.; Wang, L.; Li, X.; Zhang, J.; Che, R., MOF Induces 2D GO to Assemble into 3D Accordion-Like Composites for Tunable and Optimized Microwave Absorption Performance. *Small* **2020,** *16*, 2003905.
64. Anasori, B.; Lukatskaya, M. R.; Gogotsi, Y., 2D Metal Carbides and Nitrides (Mxenes) for Energy Storage. *Nat. Rev. Mater.* **2017,** *2*. 16098.
65. Xiang, Z.; Shi, Y.; Zhu, X.; Cai, L.; Lu, W., Flexible and Waterproof 2D/1D/0D Construction of Mxene-Based Nanocomposites for Electromagnetic Wave Absorption, Emi Shielding, and Photothermal Conversion. *Nanomicro. Lett.* **2021,** *13*, 150.
66. Guan, X.; Yang, Z.; Zhou, M.; Yang, L.; Peymanfar, R.; Aslibeiki, B.; Ji, G., 2D Mxene Nanomaterials: Synthesis, Mechanism, and Multifunctional Applications in Microwave Absorption. *Small Struct.* **2022,** *3*, 2200102.
67. Qiao, J.; Zhang, X.; Xu, D.; Kong, L.; Lv, L.; Yang, F.; Wang, F.; Liu, W.; Liu, J., Design and Synthesis of TiO_2/Co/Carbon Nanofibers with Tunable and Efficient Electromagnetic Absorption. *Chem. Eng. J.* **2020,** *380*, 122591.
68. Shu, R.; Zhang, G.; Wang, X.; Gao, X.; Wang, M.; Gan, Y.; Shi, J.; He, J., Fabrication of 3D Net-Like Mwcnts/$ZnFe_2O_4$ Hybrid Composites as High-Performance Electromagnetic Wave Absorbers. *Chem. Eng. J.* **2018,** *337*, 242-255.
69. Li, B.; Mao, B.; Wang, X.; He, T.; Huang, H., Novel, Hierarchical Sic Nanowire-Reinforced SiC/Carbon Foam Composites: Lightweight, Ultrathin, and Highly Efficient Microwave Absorbers. *J. Alloys Compounds* **2020,** *829*, 154609.
70. Zhang, Y.; Huang, Y.; Zhang, T.; Chang, H.; Xiao, P.; Chen, H.; Huang, Z.; Chen, Y., Broadband and Tunable High-Performance Microwave Absorption of an Ultralight and Highly Compressible Graphene Foam. *Adv. Mater.* **2015,** *27*, 2049-2053.
71. Chen, H.; Ma, W.; Huang, Z.; Zhang, Y.; Huang, Y.; Chen, Y., Graphene-Based Materials toward Microwave and Terahertz Absorbing Stealth Technologies. *Adv. Opt. Mater.* **2019,** *7*, 1801318.
72. Cao, M.; Han, C.; Wang, X.; Zhang, M.; Zhang, Y.; Shu, J.; Yang, H.; Fang, X.; Yuan, J., Graphene Nanohybrids: Excellent Electromagnetic Properties for the Absorbing and Shielding of Electromagnetic Waves. *J. Mater. Chem. C* **2018,** *6*, 4586-4602.
73. Wang, L.; Li, X.; Li, Q.; Yu, X.; Zhao, Y.; Zhang, J.; Wang, M.; Che, R., Oriented Polarization Tuning Broadband Absorption from Flexible Hierarchical Zno Arrays Vertically Supported on Carbon Cloth. *Small* **2019,** *15*, e1900900.
74. She, W.; Bi, H.; Wen, Z.; Liu, Q.; Zhao, X.; Zhang, J.; Che, R., Tunable Microwave Absorption Frequency by Aspect Ratio of Hollow Polydopamine@Alpha-MnO_2 Microspindles Studied by Electron Holography. *ACS Appl. Mater. Interfaces* **2016,** *8*, 9782-9789.
75. Suresh, R.; Ponnuswamy, V.; Mariappan, R., Effect of Annealing Temperature on the Microstructural, Optical and Electrical Properties of CeO_2 Nanoparticles by Chemical Precipitation Method. *Appl. Surf. Sci.* **2013,** *273*, 457-464.
76. Wu, Y.; Shu, R.; Zhang, J.; Sun, R.; Chen, Y.; Yuan, J., Oxygen Vacancy Defects Enhanced Electromagnetic Wave Absorption Properties of 3D Net-Like Multi-Walled Carbon Nanotubes/Cerium Oxide Nanocomposites. *J. Alloys Compounds* **2019,** *785*, 616-626.
77. Xu, L.; Huang, W. Q.; Wang, L. L.; Huang, G. F., Interfacial Interactions of Semiconductor with Graphene and Reduced Graphene Oxide: CeO_2 as a Case Study. *ACS Appl. Mater. Interfaces* **2014,** *6*, 20350-20357.
78. Ma, J.; Li, W.; Fan, Y.; Yang, J.; Yang, Q.; Wang, J.; Luo, W.; Zhou, W.; Nomura, N.; Wang, L.; Jiang, W., Ultrathin and Light-Weight Graphene Aerogel with Precisely Tunable Density for Highly Efficient Microwave Absorbing. *ACS Appl. Mater. Interfaces* **2019,** *11*, 46386-46396.

79. Wu, G.; Sun, S.; Zhu, X.; Ma, Z.; Zhang, Y.; Bao, N., Microfluidic Fabrication of Hierarchical-Ordered ZIF-L(Zn)@$Ti_3C_2T_x$ Core-Sheath Fibers for High-Performance Asymmetric Supercapacitors. *Angew. Chem. Int. Ed.* **2022,** *61*, e202115559.
80. Zhou, Z.; Li, P.; Man, Z.; Zhu, X.; Ye, S.; Lu, W.; Wu, G.; Chen, W., Multiscale Dot-Wire-Sheet Heterostructured Nitrogen-Doped Carbon Dots-$Ti_3C_2T_x$/Silk Nanofibers for High-Performance Fiber-Shaped Supercapacitors. *Angew. Chem. Int. Ed.* **2023,** *62*, e202301618.
81. Wu, G.; Ma, Z.; Wu, X.; Zhu, X.; Man, Z.; Lu, W.; Xu, J., Interfacial Polymetallic Oxides and Hierarchical Porous Core-Shell Fibres for High Energy-Density Electrochemical Supercapacitors. *Angew. Chem. Int. Ed.* **2022,** *61*, e202203765.
82. Wu, X.; Zhu, X.; Tao, H.; Wu, G.; Xu, J.; Bao, N., Covalently Aligned Molybdenum Disulfide-Carbon Nanotubes Heteroarchitecture for High-Performance Electrochemical Capacitors. *Angew. Chem. Int. Ed.* **2021,** *60* , 21295-21303.
83. Qing, Y.; Zhou, W.; Luo, F.; Zhu, D., Titanium Carbide (Mxene) Nanosheets as Promising Microwave Absorbers. *Ceram. Int.* **2016,** *42*, 16412-16416.
84. Deng, B.; Liu, Z.; Pan, F.; Xiang, Z.; Zhang, X.; Lu, W., Electrostatically Self-Assembled Two-Dimensional Magnetized Mxene/Hollow Fe_3O_4 Nanoparticle Hybrids with High Electromagnetic Absorption Performance and Improved Impendence Matching. *J. Mater. Chem. A* **2021,** *9*, 3500-3510.
85. Cui, Y.; Liu, Z.; Zhang, Y.; Liu, P.; Ahmad, M.; Zhang, Q.; Zhang, B., Wrinkled Three-Dimensional Porous Mxene/Ni Composite Microspheres for Efficient Broadband Microwave Absorption. *Carbon* **2021,** *181*, 58-68.
86. Cai, L.; Pan, F.; Zhu, X.; Dong, Y.; Shi, Y.; Xiang, Z.; Cheng, J.; Jiang, H.; Shi, Z.; Lu, W., Etching Engineering and Electrostatic Self-Assembly of N-Doped Mxene/Hollow Co-ZIF Hybrids for High-Performance Microwave Absorbers. *Chem. Eng. J.* **2022,** *434*, 133865.
87. Chen, F.; Zhang, S.; Ma, B.; Xiong, Y.; Luo, H.; Cheng, Y.; Li, X.; Wang, X.; Gong, R., Bimetallic CoFe-MOF@$Ti_3C_2T_x$ Mxene Derived Composites for Broadband Microwave Absorption. *Chem. Eng. J.* **2022,** *431*, 134007.
88. Liang, L.; Zhang, Z.; Song, F.; Zhang, W.; Li, H.; Gu, J.; Liu, Q.; Zhang, D., Ultralight, Flexible Carbon Hybrid Aerogels from Bacterial Cellulose for Strong Microwave Absorption. *Carbon* **2020,** *162*, 283-291.
89. Li, X.; Yin, X.; Song, C.; Han, M.; Xu, H.; Duan, W.; Cheng, L.; Zhang, L., Self-Assembly Core-Shell Graphene-Bridged Hollow Mxenes Spheres 3D Foam with Ultrahigh Specific Em Absorption Performance. *Adv. Funct. Mater.* **2018,** *28*, 1803938.
90. Shui, W.; Li, J.; Wang, H.; Xing, Y.; Li, Y.; Yang, Q.; Xiao, X.; Wen, Q.; Zhang, H., $Ti_3C_2T_x$ Mxene Sponge Composite as Broadband Terahertz Absorber. *Adv. Opt. Mater.* **2020,** *8*, 2001120.
91. Zhang, X. J.; Zhu, J. Q.; Yin, P. G.; Guo, A. P.; Huang, A. P.; Guo, L.; Wang, G. S., Tunable High-Performance Microwave Absorption of $Co_{1-x}S$ Hollow Spheres Constructed by Nanosheets within Ultralow Filler Loading. *Adv. Funct. Mater.* **2018,** *28*, 1800761.
92. Liu, Q.; Cao, Q.; Bi, H.; Liang, C.; Yuan, K.; She, W.; Yang, Y.; Che, R., CoNi@SiO_2@TiO_2 and CoNi@Air@TiO_2 Microspheres with Strong Wideband Microwave Absorption. *Adv. Mater.* **2016,** *28*, 486-490.
93. Wu, M.; Zheng, Y.; Liang, X.; Huang, Q.; Xu, X.; Ding, P.; Liu, J.; Wang, D., Mos_2 Nanostructures with the 1T Phase for Electromagnetic Wave Absorption. *ACS Appl. Nano Mater.* **2021,** *4*, 11042-11051.
94. Wu, M.; Liang, X.; Zheng, Y.; Qian, C.; Wang, D., Excellent Microwave Absorption Performances Achieved by Optimizing Core@Shell Structures of Fe_3O_4@1T/2H-MoS_2 Composites. *J. Alloys Compounds* **2022,** *910*, 164881.
95. Man, Z.; Li, P.; Zhou, D.; Wang, Y.; Liang, X.; Zang, R.; Li, P.; Zuo, Y.; Lam, Y. M.; Wang, G., Two Birds with One Stone: FeS_2@C Yolk-Shell Composite for High-Performance Sodium-Ion Energy Storage and Electromagnetic Wave Absorption. *Nano Lett.* **2020,** *20*, 3769-3777.
96. Zhang, D.; Zhang, H.; Cheng, J.; Raza, H.; Liu, T.; Liu, B.; Ba, X.; Zheng, G.; Chen, G.; Cao, M., Customizing Coaxial Stacking VS_2 Nanosheets for Dual-Band Microwave Absorption with Superior Performance in the C- and Ku-Bands. *J.Mater. Chem. C* **2020,** *8*, 5923-5933.
97. Zen. H.; Wang, H.; Huang, Z.; Zheng, Q.; Zheng, G.; Zhang, D.; Che, R.; Cao, M., Initiating Vb-Group Laminated NbS_2 Electromagnetic Wave Absorber toward Superior Absorption Bandwidth as Large as 6.48 Ghz through Phase Engineering Modulation. *Adv. Funct. Mater.* **2022,** *32*, 2108194.
98. Wu, M.; Wang, H.; Liang, X.; Wang, D., Efficient and Tunable Microwave Absorbers of the Flower-Like 1T/2H-MoS_2 with Hollow Nanostructures. *J. Alloys Compounds* **2023,** *933*, 167763.

 doi:10.20944/preprints202306.1136.v1

99. Wu, M.; Wang, H.; Liang, X.; Wang, D., Flower-Like 1T/2H-MoS_2@A-Fe_2O_3 with Enhanced Electromagnetic Wave Absorption Capabilities in the Low Frequency Range. *J. Mater. Chem. C* **2023,** *11*, 2897-2910.
100. Wu, M.; Wang, H.; Liang, X.; Wang, D., Optimized Electromagnetic Wave Absorption Ofalpha-Fe_2O_3@MoS_2 Nanocomposites with Core-Shell Structure. *Nanotechnology* **2023,** *34*, 145703.